Development 137, 4083-4090 (2010) doi:10.1242/dev.053678

Disruption of an N-acetyltransferase gene in the silkworm reveals a novel role in pigmentation

Shuai Zhan[1,2,*], Qiuhong Guo[1,*], Minghui Li[1], Muwang Li[3], Jianyong Li[4], Xuexia Miao[1] and Yongping Huang[1,†]

SUMMARY

The pigmentation of insects has served as an excellent model for the study of morphological trait evolution and developmental biology. The *melanism* (*mln*) mutant of the silkworm *Bombyx mori* is notable for its strong black coloration, phenotypic differences between larval and adult stages, and its widespread use in strain selection. Here, we report the genetic and molecular bases for the formation of the *mln* morphological trait. Fine mapping revealed that an arylalkylamine N-acetyltransferase (AANAT) gene co-segregates with the black coloration patterns. Coding sequence variations and expression profiles of AANAT are also associated with the melanic phenotypes. A 126 bp deletion in the *mln* genome causes two alternatively spliced transcripts with premature terminations. An enzymatic assay demonstrated the absolute loss of AANAT activity in the mutant proteins. We also performed RNA interference of AANAT in wild-type pupae and observed a significant proportion of adults with ectopic black coloration. These findings indicate that functional deletion of this AANAT gene accounts for the *mln* mutation in silkworm. AANAT is also involved in a parallel melanin synthesis pathway in which *ebony* plays a role, whereas no pigmentation defect has been reported in the *Drosophila* model or in other insects to date. To the best of our knowledge, the *mln* mutation is the first characterized mutant phenotype of insects with AANAT, and this result contributes to our understanding of dopamine metabolism and melanin pattern polymorphisms.

KEY WORDS: N-acetyltransferase (NAT), Pigmentation, Lepidoptera, Silkworm

INTRODUCTION

Insects exhibit the richest diversity of all animals, and the rapid evolution of their phenotypic patterns suggests strong selective forces that promote and maintain variation. As a prototype of visible variation in insects (True, 2003), the melanism phenomenon is one of the most commonly cited examples of natural selection in evolutionary biology (Koch et al., 2000) relating to industrial pollution or mimicry. Melanism is generally characterized as the result of ectopic melanin deposition. In most invertebrates, melanin synthesis is achieved by the phenoloxidase (PO)-activating system and is crucial in many biological processes, including innate immunity, sclerotization and pigmentation pathways (Ashida and Brey, 1995; Soderhall and Cerenius, 1998; Andersen, 2005). As an initial step in this biochemical cascade, toxic quinone intermediates and *o*-quinones are produced, which can damage the hosts (Andersen, 2005; Kan et al., 2008). PO-induced melanin synthesis must therefore be tightly controlled to avoid deleterious pleiotropic effects on normal development and coloration.

The adult *melanism* (*mln*) body of the silkworm *Bombyx mori* shows strong overall pigmentation, whereas the wild type does not (Fig. 1A). However, black coloration appears only on the head, forelegs and tail spot of larval *mln* mutants, areas that are colorless in wild-type larvae (Fig. 1B). This striking phenomenon is of considerable interest in the investigation of the mechanism of fine-scale regulation of pigment metabolism and morphological divergence.

The melanin patterns of fruit flies provide useful models for understanding the evolution of morphology and spatial gene regulation (Wittkopp et al., 2003a; Carroll, 2005; Wray, 2007; Jeong et al., 2008; Wittkopp et al., 2009). Lepidoptera is a large order of insects that includes numerous agricultural and forest pests. A wide variety of markings and patterns, including many unique phenotypes not observed in the *Drosophila* model, facilitate the avoidance of natural enemies. Detailed characterization of such polymorphisms might lead to a broader understanding of selective mechanisms. Within lepidopteran species, the silkworm is considered a suitable model for the genetic and molecular identification of traits owing to its substantial economic value (Fujii et al., 1998; Goldsmith et al., 2005), abundantly maintained variants and widely available genetic and genomic resources (Mita et al., 2004; Xia et al., 2004; Miao et al., 2005; International Silkworm Genome Consortium, 2008; Yamamoto et al., 2008; Zhan et al., 2009). Recently, several larval mutants have been identified for this well-studied model (Futahashi et al., 2008; Ito et al., 2009; Meng et al., 2009b; Ito et al., 2010), including novel models outside of the classical insect melanin synthesis pathway (Ito et al., 2009; Meng et al., 2009b).

Here we report the molecular identification of the silkworm *mln* locus by scoring backcross progeny. The putative mutation mechanism was also verified by enzymatic assay and RNA interference (RNAi) phenotypes. We conclude that the black coloration of the adult correlates with the loss of arylalkylamine N-acetyltransferase (AANAT) activity by frameshift mutation. Our evidence describes, for the first time, the pigmented phenotype of an enzyme that has long been known, in principle, to function in pigment synthesis (Fig. 1). This is also the first time that RNAi has been used to support linkage analyses in moth.

[1]Institute of Plant Physiology and Ecology, Shanghai Institutes for Biological Sciences, Chinese Academy of Sciences, Shanghai, 200032, China. [2]The Graduate School, Chinese Academy of Sciences, Shanghai, 200031, China. [3]Sericultural Research Institute, Chinese Academy of Agriculture Sciences, Zhenjiang, 212018, China. [4]Virginia Polytechnic Institute and State University, Blacksburg, VA 24061, USA.

*These authors contributed equally to this work
†Author for correspondence (yphuang@sibs.ac.cn)

Accepted 23 September 2010

MATERIALS AND METHODS

Silkworm strains

As *mln* is a recessive single locus trait, we designed crosses based on the single-pair backcross model (Miao et al., 2005). The *mln* strain *i04* was crossed with the wild-type strain *Dazao*. The resulting female F1 and male F1 were backcrossed with *i04* to generate BC1F and BC1M populations, including 22 BC1F individuals (12 were wild type, ten were black) and 171 BC1M individuals (92 were wild type, 79 were black). Because the silkworm lacks crossing over in females (Maeda, 1939), the BC1F population was used to determine the linkage group and to screen for polymorphisms.

Additional wild-type (*C108*, *Jingsong*, *Lan10*, *Nistari*, *Hua8*, *D1.31*, *D24.98* and *Hainanmj*) and *mln* (*i04*, *Tchi*, *Huayuan*, *1AHz03*, *1AHD1.31* and *z03*) strains were used to detect and confirm the genotypes. All strains are preserved in the Zhenjiang Sericultural Research Institute of the Chinese Academy of Agricultural Sciences.

Sample preparation

Silkworms were fed with fresh mulberry and reared at 25°C. Whole bodies of individuals were homogenized in liquid nitrogen or with stainless steel drills, then genomic DNA was extracted as described (Zhan et al., 2009) and total RNA was isolated using TRIzol (Invitrogen) according to the manufacturer's protocol. ReverTra Ace-α (TOYOBO) was used for cDNA reverse transcription.

Linkage mapping and candidate gene screening

Our previously developed simple sequence repeat (SSR) markers (Miao et al., 2005; Zhan et al., 2009) were screened in BC1F, and the co-segregated markers were then genotyped in the BC1M population as described (Miao et al., 2005). Linkage maps were generated by MAPMAKER/EXP 3.0b (Lander et al., 1987) using the Kosambi function as described (Zhan et al., 2009). SilkDB (Duan et al., 2010) was used to localize the markers according to the flanking sequences, and subsequently used to predict the candidate genes based on their GLEAN model (Elsik et al., 2007; International Silkworm Genome Consortium, 2008). Open reading frames (ORFs) of candidates were cloned into pMD18-T vectors (TAKARA) and sequenced using a 3730 DNA analyzer (Applied Biosystems) with three independent replicates. Spatial expression profiles of candidate genes were obtained from the BmMDB database (Xia et al., 2007) and temporal profiles (available from GEO with accession GSE24611) were determined by the Agilent 8X15K gene expression platform. Insects were sampled daily in the larval and pupal stages. Total RNA of each sample was extracted separately and then mixed equally as egg, larva, pupa and adult samples for RNA amplification and labeling. A total of 14,623 silkworm genes for designing probes were derived from the GLEAN gene model (International Silkworm Genome Consortium, 2008). Oligonucleotide probe design, microarray construction, RNA labeling and hybridization, microarray imaging and data processing were performed by Shanghai Biochip (China).

Analysis of sequences and expression profiles

Quantitative real-time PCR was performed with SYBR Premix Ex Taq (TAKARA) on a Rotor-Gene 3000 real-time thermal cycler (Corbett Research) as described (Huang et al., 2007). BmG3PDH was amplified as the control to standardize the amount of cDNA. Primers are listed in Table S1 in the supplementary material. Annotation of candidate genes was carried out via the NCBI BLASTX (http://blast.ncbi.nlm.nih.gov/Blast.cgi) and the InterProScan (http://www.ebi.ac.uk/Tools/InterProScan) online platforms. AANAT family protein sequences were collected from GenBank (http://www.ncbi.nlm.nih.gov/Genbank). Identification numbers for the proteins used in Fig. S2 in the supplementary material are as follows: *Arabidopsis thaliana*, NP_563677; *Antheraea pernyi*, ABD17803; *Apteryx australis*, AAQ17197; *Bacillus subtilis*, NP_388474; *Bombyx mori*, NP_001073122; *Bos taurus*, NP_803475; *Caenorhabditis elegans*, NP_501392; *Canis familiaris*, ABC74871; *Chlamydomonas reinhardtii*, BAH10512; *Coturnix coturnix*, AAB62871; *Culex quinquefasciatus*, EDS43162; *Danio rerio*, NP_956998; *Dicentrarchus labrax*, ACB13284; *Dictyostelium discoideum*, P36416; *Drosophila melanogaster*, CAA69262; *Escherichia coli*, NP_290986; *Gallus gallus*, NP_990489; *Homo sapiens*, NP_001079; *Macaca mulatta*, NP_001040592; *Mus musculus*, NP_033721; *Mycobacterium tuberculosis*, NP_217937; *Neurospora crassa*, EAA32826; *Oncorhynchus mykiss*, NP_001117729; *Oryzias latipes*, BAE78760; *Ovis aries*, NP_001009461; *Pan troglodytes*, NP_001012442; *Periplaneta americana*, BAC87874; *Pezoporus occidentalis*, ABJ98438; *Podargus strigoides*, AAR32944; *Rattus norvegicus*, NP_036950; *Saccharomyces cerevisiae*, NP_010356; *Scyliorhinus canicula*, ACB13283; *Streptococcus pneumoniae*, NP_345969; *Sturnus vulgaris*, AAP94214; and *Xenopus laevis*, AAP57669. Multiple alignments were performed and a UPGMA phylogenetic tree was generated by MEGA 4 (Tamura et al., 2007).

Protein expression, purification and detection

Prokaryotic expression of recombinant protein was performed as follows. The intact ORFs (predicted for lm and sm) were cloned into pET-22b (Novagen) fused with a C-terminal hexa-histidine tag (6×HIS), the recombinant vectors were confirmed and transformed into *E. coli* DE3, and fusion proteins were expressed after IPTG induction at 37°C. An additional approach for expression of lm included another donor vector, pGEX-4t-3 (GE Healthcare), fused with glutathione S-transferase (GST). The recombinant protein was also expressed in Sf9 insect cells using a Bac-to-Bac baculovirus expression system (Invitrogen). pFastBac HT-A constructs containing intact corresponding ORFs and 6×HIS were generated and transformed into DH10Bac *E. coli* for transposition into the bacmids. Cellfectin (Invitrogen) was used for transfection of Sf9 cells with the confirmed recombinant bacmid. The third generation of the amplified recombinant baculovirus stock was used to infect Sf9 cells to express the recombinant protein. *E. coli* or cell pellets were rinsed and resuspended in 1× PBS, then homogenized by sonication in lysis buffer (pH 7.5) comprising 20 mM HEPES, 20 mM NaOH, 1 mM EDTA, 1 mM DTT, 100 μg/ml PMSF, 10% glycerol, 0.01% Nonidet P40 and Protease Inhibitor Cocktail (GE Healthcare). The samples were centrifuged at 16,000 rpm (28,672 ***g***) for 20 minutes at 4°C, and then the recombinant proteins were purified from the supernatant using Ni-NTA Superflow cartridges (Qiagen). Proteins were eluted with Tris-HCl buffer (50 mM Tris, 100 mM NaCl, pH 7.5) for enzymatic assay.

Recombinant proteins were separated by 12% SDS-PAGE at 80 mA for 2 hours. Western blotting was performed by semi-dry transfer to Hybond-C nitrocellulose membrane (Amersham Biosciences) for 90 minutes at 0.8 mA/cm^2. Each membrane was then treated as follows: (1) blocked with 5% milk in TBST (2.5 mM Tris, 15 mM NaCl, 0.2 mM KCl, 0.1% Tween 20, pH 7.4) with gentle shaking for 3 hours; (2) incubated in mouse anti-HIS antibody (1:3000 dilution, Sigma) at 4°C overnight; (3) washed three times in TBST with gentle shaking for 10 minutes; (4) incubated in TBST with a 1:1000 goat HRP-conjugated anti-mouse IgG (H+L) antibody (Proteintech Group) at 4°C for 1 hour; and (5) washed three times in TBST with gentle shaking for 10 minutes. HRP activity was detected using a chemiluminescent substrate (Millipore), and the films and blots were imaged using a Kodak 102 medical X-ray processor.

AANAT activity assay

The assay procedure employed standard protocols (Borjigin et al., 1995; Ichihara et al., 2001) with some modification. The 25 μl reaction mixture contained 0.5 μl 50 mM tryptamine or dopamine (Sigma-Aldrich), 5 μl 5 mM acetyl-CoA [10 mM H^3-labeled (PerkinElmer) mixed with 5 mM unlabeled (Sigma-Aldrich) acetyl-CoA to give 1:3 hot:cold], purified protein and Tris-HCl buffer. After incubation at 37°C for the appropriate time, the reaction was stopped by adding 125 μl 5% acetic acid. Then, 600 μl of a toluene/isoamyl alcohol mixture was added (97:3 for the tryptamine substrate, 3:2 for the dopamine substrate), followed by 30 seconds of vortexing and a 5-minute centrifugation at 800 ***g***. Then, 400 μl of the organic phase was transferred to a scintillation vial containing 1.2 ml liquid scintillation cocktail (PerkinElmer). Radioactivity was measured with a liquid scintillation counter (LS-6500, Beckman).

RNAi

For RNAi experiments, double-stranded (ds) RNAs were synthesized from PCR templates using the MEGAscript T7 Transcription Kit (Ambion) according to the manufacturer's protocol. Primers used to generate PCR templates contained a T7 promoter at the 5′ end, and the amplified regions corresponded to cDNA of nucleotides 133-536 of C11 and 57-596 of C12. Injection of dsRNA into pupae (day 4 or 5) was performed as described

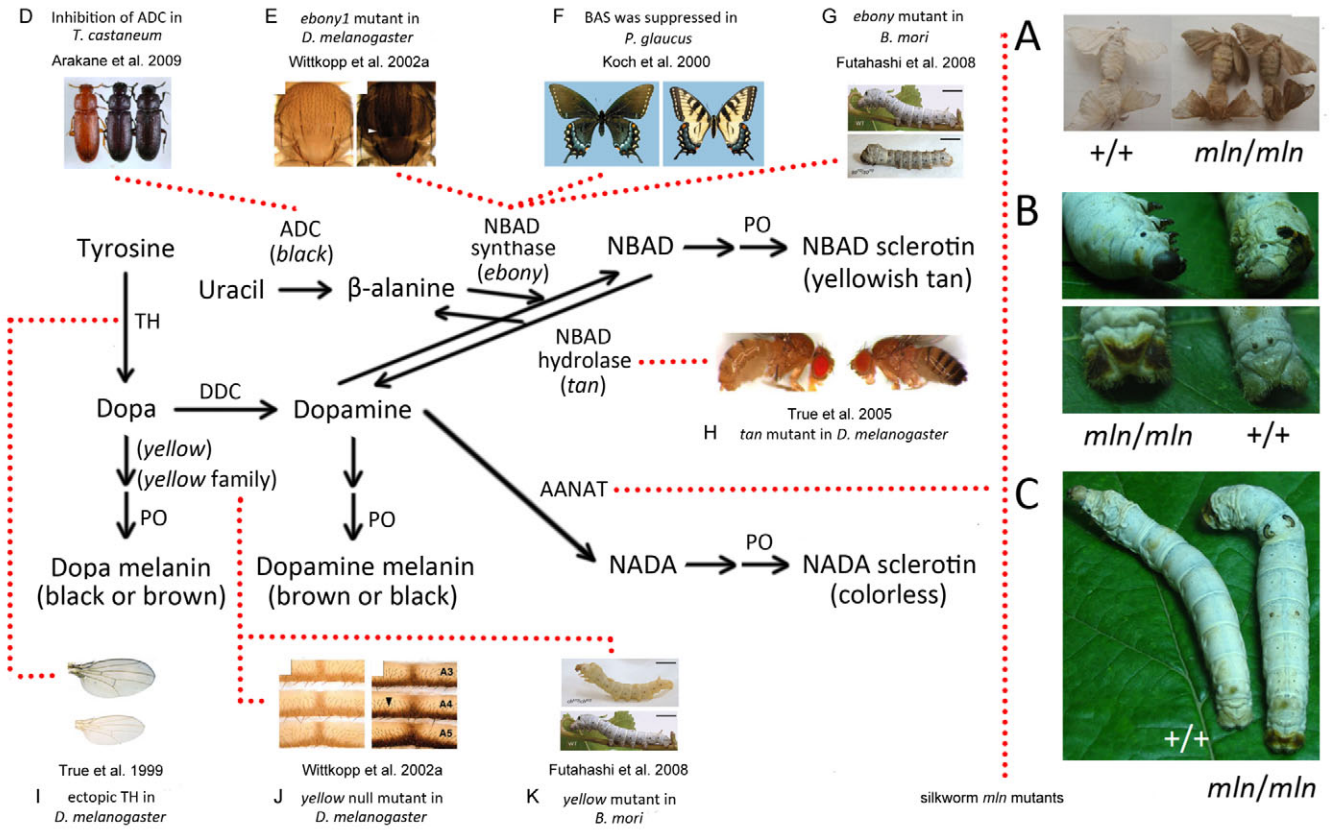

Fig. 1. Insect pigmentation pathway and melanin synthesis enzyme-induced phenotypes. The proposed insect pigmentation pathway [largely according to published literature (True, 2003; Wittkopp et al., 2003a; Arakane et al., 2009)] is illustrated in the center (see Discussion). (**A**) Adult wild-type (+/+) and *mln* mutant (*mln*/*mln*) *Bombyx mori*. (**B**) Regional pigmentation phenotypes of *mln* and wild-type larvae. In *mln*, the head and forelegs are intensely black and the tail spot is brown, instead of colorless as in the wild type. (**C**) The *mln* locus has been introduced into a line for silk production. The left larva is *Jingsong*, a traditional high-yielding strain in China. (**D-K**) According to published reports, several representative phenotypes of insects are presented as follows: (D) the middle specimen indicates *Tribolium castaneum* injected with dsRNA for ADC, and the right-hand specimen indicates the *T. castaneum* black mutant [reproduced with permission (Arakane et al., 2009)]; (E) on the right, the thorax phenotype of the *D. melanogaster ebony*^{1} mutant [reproduced with permission (Wittkopp et al., 2002a)]; (F) on the left, NBAD synthase (BAS) activity is suppressed, resulting in a melanic female *Papilio glaucus* phenotype [reproduced with permission (Koch et al., 2000)]; (G) the phenotype of the *B. mori so* mutant is shown below and is determined by the deletion of the silkworm *ebony* gene [reproduced with permission (Futahashi et al., 2008)]; (H) the phenotype of the *D. melanogaster tan*^{5} mutant is shown on the right [reproduced with permission (True et al., 2005)]; (I) ectopic melanin pattern typical of *hsp70-GAL4/+*; *UAS-TH/+* (ectopic tyrosine hydroxylase) flies is shown above [reproduced with permission (True et al., 1999)]; (J) on the left is the thorax of a *D. melanogaster yellow* mutant [reproduced with permission (Wittkopp et al., 2002a)]; (K) the top specimen indicates the *B. mori ch*^{k12} mutant caused by a *yellow* mutation [reproduced with permission (Futahashi et al., 2008)]. The insects in D-K not specifically mentioned above are wild type. Our findings provide the first model of an arylalkylamine N-acetyltransferase (AANAT) mutation contributing to an ectopic color pattern. Red dotted lines connect pairs of enzymes and their corresponding phenotype. ADC, amino acid decarboxylases; DDC, DOPA decarboxylase; LM, long mutant; NADA, *N*-acetyl dopamine; NBAD, *N*-β-alanyl dopamine; PO, phenoloxidase.

(Huang et al., 2007). dsRNA for enhanced green fluorescent protein (EGFP, from Clontech pEGFP-N1, nucleotides 74-619) was used as a control. Ten insects (five male and five female) were sampled as a group for analysis of gene expression at 0, 24, 48 and 72 hours after injection by real-time PCR, as described above.

RESULTS

Mapping the *mln* locus of *Bombyx mori*

We initially screened polymorphisms from 518 SSR markers within the female backcross BC1F population. The genotyping results demonstrated that the markers on chromosome 18 co-segregated with the black color trait, which was consistent with previous results (Miao et al., 2005). Eight available markers (see Table S1 in the supplementary material) on chromosome 18 were then genotyped on 171 BC1M segregants. Based on the linkage analysis (LOD=5), we localized the mutation site between S1808 and S1807 (Fig. 2A). These two closely linked markers corresponded to 8,223,821 and 8,871,281 bp, respectively, of nscaf2902 according to the SilkDB database (Duan et al., 2010) (Fig. 2B). Thus, the candidate region was narrowed to ~650 kb.

Identification of the *mln* candidate gene

A total of 13 predicted genes were found in the region of interest (Fig. 2C and see Table S2 in the supplementary material). Based on comparisons of coding sequences, seven candidates were excluded (Fig. 2C): C2, C12 and C13 of *mln* (*b04*) were identical to those in the wild-type strain *Dazao*; C3 and C6 only exhibited several silent SNPs, using *Dazao* as a reference; and SNPs detected in C1 and C8 appeared specific to *Dazao*, as *mln* shared the same genotype at these sites with another wild-type strain, *Jingsong*. We also detected an insertion in C7 of *mln* but not *Dazao*, but this mutation was found not to be *mln* specific after more wild-type and

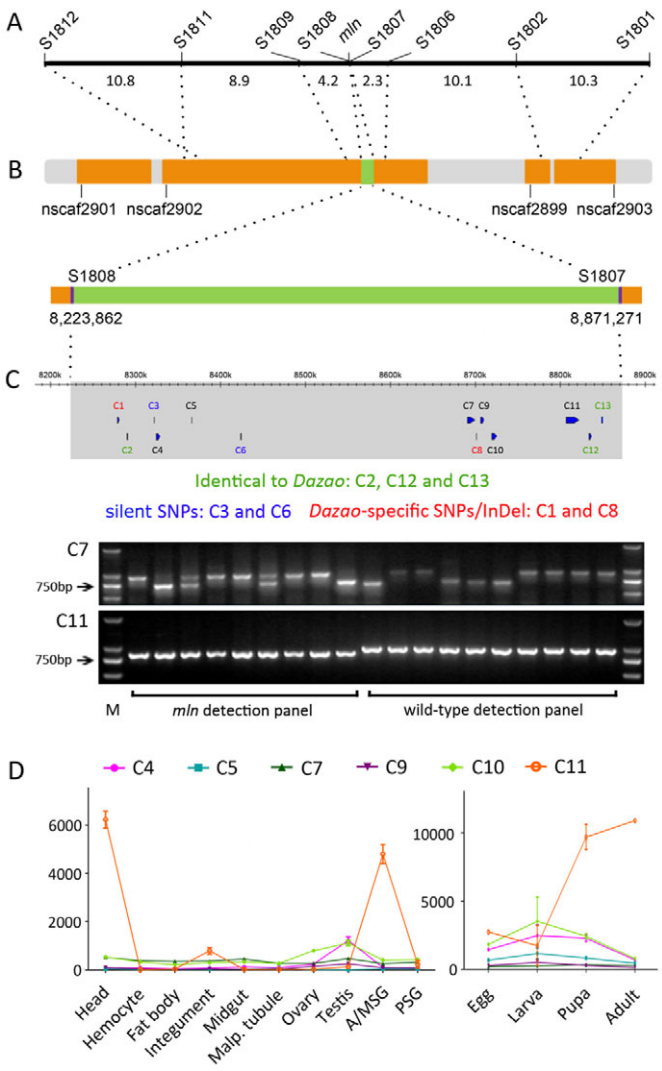

Fig. 2. *mln* mapping on *Bombyx mori* chromosome 18 and identification of candidate genes. (**A**) A linkage map based on BC1M genotyping was constructed for group 18. Eight available simple sequence repeat (SSR) markers and the *mln* locus are shown above the map. Distances between loci (cM) are shown below the map. (**B**) Scaffold map of chromosome 18, based on data from the SilkDB database. Orange boxes represent the assembled scaffolds, the names of which are given beneath. The SSR markers used for genotyping are localized on the scaffold positions, as indicated by the dotted lines. The green box shows the candidate region linked to the *mln* locus. The enlarged candidate region is shown beneath along with the position on nscaf2902 of S1807 and S1808, which fix the candidate region. (**C**) Above is shown the coordinates of nscaf2902. The gray area represents the candidate region, which includes 13 predicted genes according to SilkDB. For convenience, they are named C1 to C13 based on their position. Detailed information for these 13 genes is given in Table S2 in the supplementary material. The seven genes labeled in color were excluded for the reasons given beneath. Beneath are shown PCR polymorphism patterns of C7 and C11. The detection panel used DNA from fifth instar day 3 larvae as follows (from left to right): *Tchi*, *Huayuan*, *z03* (male), *z03* (female), *1AHz03* (male), *1AHz03* (female), *1AHD1.31* (male), *1AHD1.31* (female), and *i04* in the *mln* panel and *Dazao*, *C108*, *Jingsong*, *Lan10*, *Nistari*, *Hainanmj*, *Hua8*, *D24.98*, *D1.31* (male) and *D1.31* (female) in the wild-type panel. M is a DNA marker, showing (top to bottom) 2000, 1000, 750 and 500 bp. (**D**) Expression profiles of the remaining six candidates. The left graph presents the expression values in multiple silkworm tissues on the third day of the fifth instar (Xia et al., 2007), whereas the right graph shows expression values in four developmental stages based on microarray data (GSE24611). Bars indicate mean ± s.d. of replicates. Malp. tubule, malpighian tubule; A/MSG, anterior and middle silk gland; PSG, posterior silk gland.

mln strains were examined. In addition to the sequence variations, the expression pattern of the candidate gene should associate with substantial expression on the larval head and tail spot, and over the entire body of the adult (Fig. 1A,B). Based on available microarray data (Xia et al., 2007), both stage- and tissue-specific expression profiles suggested that candidates C4, C5, C7, C9 and C10 could be excluded because of their unrelated patterns (Fig. 2D). Sequence analysis revealed a 126 bp deletion in C11 in the *mln* genomes (Fig. 2C) and the level of C11 transcripts was significantly elevated in adult stages and relatively high in the head and integument (Fig. 2D), providing a basis for predicting that mutation of C11 is responsible for the observed phenotype. Using real-time PCR, we further investigated the expression pattern of C11, including in the tail spot. As expected, C11 was strongly expressed in the head, integument and tail spot (see Fig. S1 in the supplementary material), where black coloration was evident in the larvae of *mln* strains.

Sequence analysis of *mln*

According to the annotation, C11 represents *Bm*-iAANAT, a previously cloned silkworm gene that encodes an AANAT (Tsugehara et al., 2007). *Bm-iAANAT* consists of five exons and spans a ~3.9 kb region on nscaf2902 (Fig. 3A). Genomic sequencing of *mln* revealed a 126 bp deletion of the distal part of exon 4 and the beginning of the next downstream intron, and a 30 bp tandem insertion of the following 30 bp sequence (Fig. 3B). We obtained cDNA from *mln* mutants and identified two co-existing transcripts in various strains and stages (Fig. 3C). The short mutant (sm) ORF (deposited in GenBank with accession GU479039) was spliced from exon 3 to exon 5 and completely lacked exon 4, whereas the long mutant (lm) ORF (deposited in GenBank with accession GU479038) contained the defective exon 4 and an additional 15 bp from the downstream intron (Fig. 3C). Based on the GT/AG rule, we believe that the lack of the original splice site and the import of GT from the following 15 bp insertion are likely to have resulted in alternative splicing, a pattern that has been observed previously in another silkworm mutant (Futahashi et al., 2008).

Wild-type *Bm-iAANAT* encodes 261 amino acids, with a putative GCN5-related N-acetyltransferase domain (IPR000182, InterProScan) at residues 53-259 and a coenzyme A-binding pocket structure (cd04301, NCBI BLASTX) at residues 180-195 (Fig. 3C). In the *mln* mutant, the deletion in exon 4 caused the frameshift mutations for sm and lm from residues 132 and 179, respectively. Multiple alignments suggest that both of these mutated proteins most likely lack the function of the wild-type.

Phylogenetic analysis of AANAT

AANAT genes have been cloned in many organisms (Klein, 2007; Tsugehara et al., 2007). They have generally been reported as penultimate, rate-limiting enzymes in the reaction of serotonin with acetyl-CoA to form N-acetylserotonin, playing a major role in the regulation of melatonin circadian rhythm in vertebrates (Ferry et al., 2000). However, *Drosophila melanogaster* AANAT1 (*Dat*)

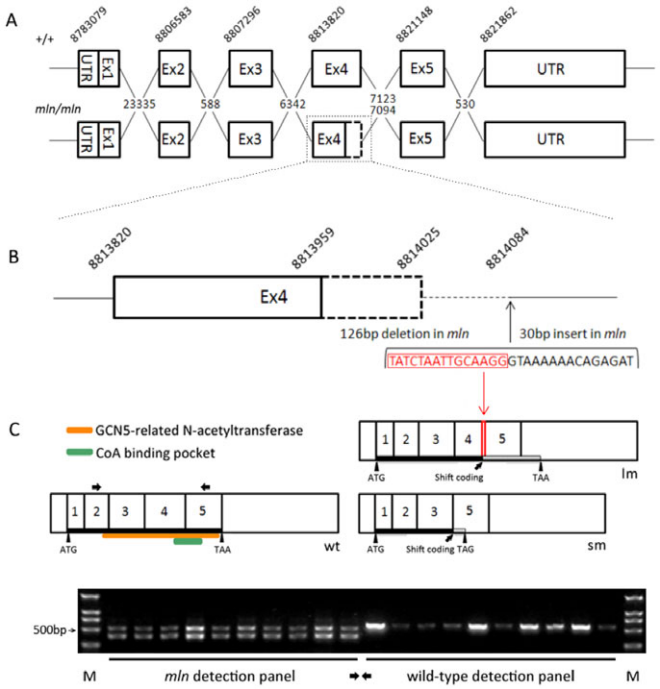

Fig. 3. Differences in *Bm-iAANAT* between the wild type and *mln*. (**A**) Boxes indicate the exons (Ex) of *Bm-iAANAT*; the positions of their start points on nscaf2902 are shown above. The lines connecting boxes indicate introns, and the numbers represent their length. A deletion in *mln* was found in exon 4 and the next downstream intron, as indicated by the dotted box and the shortened length of the intron. (**B**) An enlarged view of the deletion region. The 126 bp deletion in the *mln* genome is indicated by dotted lines. The positions of the start point of exon 4, the start point of the deletion, the point of the original splice junction, and the end point of the deletion are shown above. An additional 30 bp insertion into the *mln* genome is marked by brackets and its base sequence shown. (**C**) *Bm-iAANAT* transcripts in the wild type and *mln*. Two parallel transcripts in *mln*, termed lm and sm, are indicated by the splicing of exon boxes. The red box indicates the *mln*-specific insertion from the red base portion of the insertion in the genome as shown in B. The black rectangles crossing the exon boxes indicate the *Bm-iAANAT* coding sequences (CDSs), and the gray rectangles indicate the altered protein sequences caused by a frameshift mutation. A GCN5-related N-acetyltransferase domain (orange) and the conserved CoA-binding pocket (green) are highlighted. The PCR patterns of the transcripts in *mln* and wild-type are shown beneath. The primer set used for amplification is indicated by the pair of black arrowheads above the boxes. The detection panel used cDNA from fifth instar day 3 larvae as follows (from left to right): *Tchi*, *Huayuan*, *z03* (male), *z03* (female), *1AHz03* (male), *1AHz03* (female), *1AHD1.31* (male), *1AHD1.31* (female), *i04* and *i04* (adult) in the *mln* panel and *Dazao*, *C108*, *Jingsong*, *Lan10*, *Nistari*, *Hainanmj*, *Hua8*, *D24.98*, *D1.31* (male) and *D1.31* (female) in the wild-type panel. M is a DNA marker, showing (top to bottom) 2000, 1000, 750 and 500 bp.

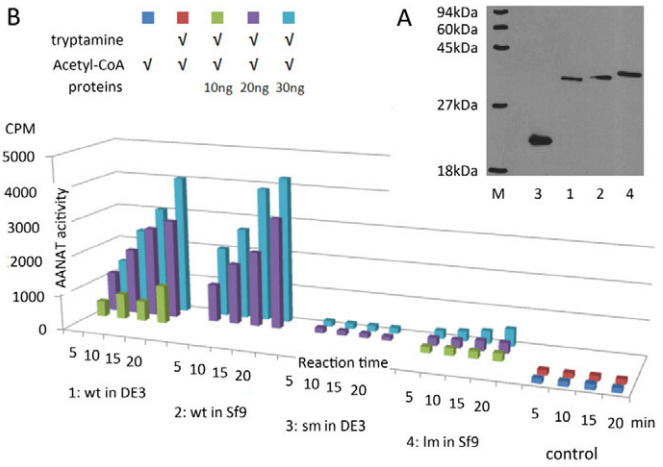

Fig. 4. Expression of recombinant Bm-iAANAT and differences in enzymatic properties between wild-type and mutant proteins. (**A**) The recombinant proteins were detected by western blotting using HIS antibody. M, molecular weight marker; 1, purified recombinant wild-type (wt) protein expressed in *E. coli*; 2, purified recombinant wt protein expressed in Sf9 cells; 3, purified recombinant sm protein expressed in *E. coli*; 4, purified recombinant lm protein expressed in Sf9 cells. (**B**) AANAT activity of the recombinant proteins and control set. Color coding indicates the amounts of recombinant protein in a standard reaction. Negative controls with and without substrate are represented by red and dark blue, respectively. Radiolabeled raw data values are presented in Table S3 in the supplementary material.

represents a novel gene family that is unrelated to known acetyltransferases, except for two weakly conserved amino acid motifs (Hintermann et al., 1996). Our phylogenetic analysis, based on amino acid sequences of AANAT, showed that the Chinese tussah moth (*Antheraea pernyi*) enzyme exhibits the highest degree of homology with the silkworm enzyme. Independent insect clusters were derived from Protista and were subsequently well separated from vertebrate lineages (see Fig. S2 in the supplementary material), which suggests the novel role of AANAT in insects. This evolutionary pattern is consistent with that of genes responsible for other visible silkworm traits, such as *BmKYNU*, a kynureninase gene that determines the *red blood* (*rb*) mutant (Meng et al., 2009a).

Enzymatic properties of Bm-iAANAT in *mln*

The phylogenetic analysis suggests that AANAT might have additional functional domains. To further investigate the enzymatic properties of Bm-iAANAT in *mln* mutants, we expressed three recombinant proteins and compared AANAT activity between normal (wt) and two mutant (lm and sm) types. Overexpression of wt and sm was detected in a bacterial expression system; however, expression of lm was not observed. Therefore, we used Sf9, a cell line derived from pupal ovarian tissue of *Spodoptera frugiperda*, to produce this mutant protein. SDS-PAGE and immunoblot analysis demonstrated that the sizes of the purified proteins were exactly as predicted (Fig. 4A). The relative molecular mass of the bacterially expressed lm recombinant protein was slightly lower than that expressed in insect cells, indicating some post-translational modification in eukaryotic cells.

We assayed wt and mutant recombinant AANAT proteins for AANAT activity using tritium-labeled acetyl-CoA and tryptamine as substrates. Radiolabeled product formation was proportional to the incubation time and the amount of protein in the reaction mixtures containing wt recombinant protein. By contrast, the AANAT activity of sm and lm remained significantly lower, even when the amount of protein or reaction time was greatly increased (Fig. 4B and see Table S3 in the supplementary material). We also used dopamine, another monoamine, as a substrate for the enzymatic assay, and this confirmed the inactivity of AANAT in

Table 1. Phenotypic counts for the C11 RNAi experiment

Treatment (10 μg)	Gender	Injected	Molted				Death
			Total	R	O	No	
dsAANAT	All	212	208	107	54	47	4
	Male	100	96	72	18	6	4
	Female	112	112	35	36	41	0
dsEGFP	All	100	97	0	0	97	3

R, regional melanization; O, overall melanization; No, no ectopic phenotype.

sm and lm (see Table S4 in the supplementary material). These data demonstrate that the mutation of *Bm-iAANAT* in *mln* causes the associated loss of function.

RNAi verification

The entire body of *mln* adults is black. To verify whether a deficiency of Bm-iAANAT is responsible for the black color pattern of the integument, we performed RNAi experiments to suppress the expression of the corresponding gene in wild-type insects. After injecting dsAANAT into pupae, we observed that the cuticle of the majority of wild-type adults (90 of 96 males and 71 of 112 females; Table 1) turned partly (Fig. 5A,B) or completely (Fig. 5B-E) black. It is conceivable that the phenotype produced by RNAi-mediated repression of C11 is less severe than that caused by the *mln* mutation. We also noticed that RNAi of C11 was more effective with males than females. In the RNAi experiment, we injected equal amounts of dsRNA into female and male pupae, but because the male pupae are usually smaller than female pupae, the males effectively received a higher dose, causing the effect of RNAi to be more evident. Real-time PCR revealed that the level of *Bm-iAANAT* transcription was significantly downregulated on the third day after dsRNA injection (Fig. 5F). We also injected dsAANAT into *mln* mutants, but observed no change in the melanic phenotype. These findings provide additional evidence that the black coloration of *mln* results from the loss of its AANAT function.

DISCUSSION

Dat is reported to be involved in melanin metabolism rather than in time keeping (Wright, 1987; Wittkopp et al., 2003a; Wittkopp et al., 2003b). In this process (Fig. 1), tyrosine is hydroxylated to DOPA by tyrosine hydroxylase (TH), and DOPA can then be transformed into dopamine by decarboxylation by DOPA decarboxylase (DDC). Dopamine is a key compound for both sclerotization and melanin formation (Andersen, 2005). The black color patterns of insects are the result of ectopic melanin deposition, which reflects the differential spatial regulation of four parallel branches from the core dopamine pathway (Wright, 1987; True et al., 1999; Wittkopp et al., 2002a). The downstream products of dopamine – *N*-acetyl dopamine (NADA) and *N*-β-alanyl dopamine (NBAD) – can both serve as precursors in cuticle sclerotization (True, 2003; Wittkopp et al., 2003a), as an alternative to producing DOPA-melanin or dopamine-melanin pigments (Fig. 1). For decades, fruit fly pigmentation studies have focused on *ebony* (Wittkopp et al., 2002a; Kohn and Wittkopp, 2007; Wittkopp et al., 2009) and *tan* (True et al., 2005; Jeong et al., 2008; Wittkopp et al., 2009), which are involved in the NBAD branch that inhibits melanin formation (Fig. 1), or on *yellow* (Wittkopp et al., 2002a; Wittkopp et al., 2002b; Gompel et al., 2005), which is involved in branches that promote melanin formation (Fig. 1). Several ectopic phenotypic traits for upstream enzymes, such as TH and DDC, have also been identified in the Swallowtail butterfly and Red flour beetle (Koch et al., 2000; Futahashi and Fujiwara, 2005; Arakane et al., 2009). In a parallel pathway to *ebony*, AANAT catalyzes the conversion of dopamine to NADA, but no mutant phenotype has been observed (Brodbeck et al., 1998). AANAT was previously considered to have a major role in sclerotization (Walter et al., 1996; Andersen, 2005; Gibert et al., 2007). We provide the first phenotypic demonstration of the contribution of AANAT to insect color patterns.

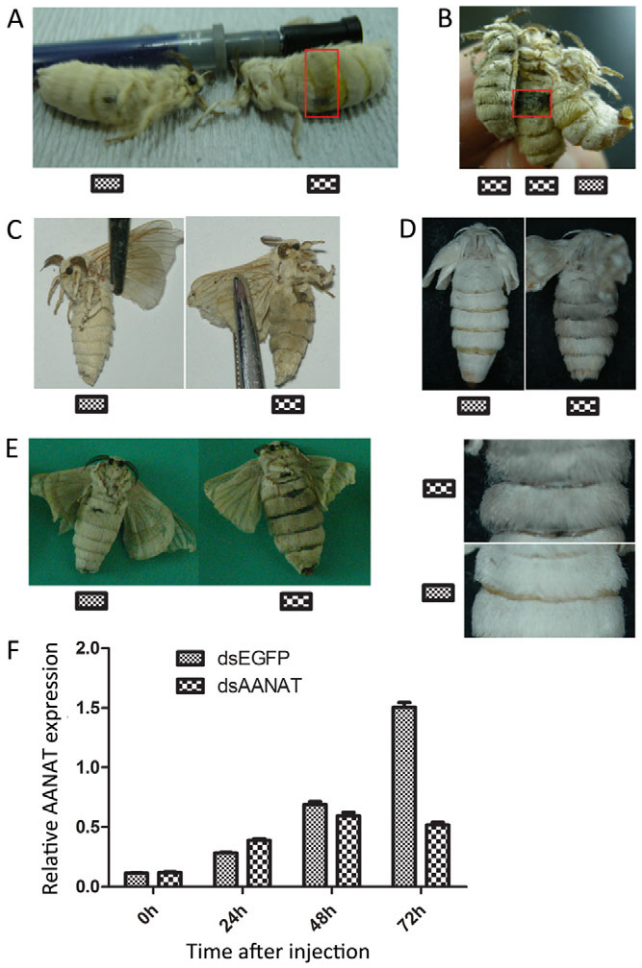

Fig. 5. Effect of RNAi on Bm-iAANAT. (**A-E**) After injecting dsAANAT into pupae, the cuticle of the majority of wild-type adults turned partly (A,B; the ectopic portion is boxed in red) or completely (B-E) black. An enlarged view of regional segments is shown in D, below. dsEGFP-injected controls are shown for comparison. (**F**) *Bm-iAANAT* expression levels are shown for the four time points following dsRNA injection. The relative AANAT expression level in dsAANAT-treated and dsEGFP-treated (control) insects is presented relative to the level of *BmG3PDH*. Mean ± s.d.

Taking into account the previous lines of phenotypic evidence, the mutation of each gene in the melanin synthesis pathway appears to confer a unique or complex color pattern in insects. Many or all of the genes involved are pleiotropic, as melanism has roles in multiple parts of the body and in other physiological processes, such as innate immunity and development. Thus, the independent and stable phenotypic defects are likely to be due to functional redundancy among the gene family members in insects. Recent research has shown that the yellow-e protein determines the silkworm *bts* mutant (Ito et al., 2010), which exhibits a similar

phenotype to *mln* larvae. However, our results show that the *mln* (*b04*) *Bmyellow-e* cDNA sequence is identical to that of the wild type, suggesting that they share a similar function in shaping silkworm larval pigmentation.

In the candidate region, C12, another NAT gene, is located adjacent to the candidate in *mln*, which raises the question of whether a defect of C12 might be responsible for the observed *mln* phenotype. We initially excluded C12 because of the lack of a coding mutation, but recent published work has shown evidence for regulatory mutation in the silkworm trait (Sakudoh et al., 2010). Comparative analysis indicated that the expression levels of C12 at the sites where melanism was seen (such as the larval head, the larval tail spot and the whole body of the adult) were essentially the same in the wild type and *mln* mutant (see Fig. S3A in the supplementary material). This would seem to preclude the possible occurrence of regulatory mutations in C12. In addition, we did not find a correlation between the expression pattern of C12 and the melanic phenotypes of mutants (see Fig. S3B,C in the supplementary material), which reinforces the notion that C12 is not related to the *mln* phenotype. RNAi of C12 in wild-type insects effectively suppressed C12 expression (see Fig. S4 in the supplementary material), but this did not lead to any ectopic melanic phenotype (see Table S5 in the supplementary material). Taken together, these data provide a sufficient basis to exclude the involvement of C12 in the *mln* phenotype.

mln phenotypes differ between larvae and adults within the same strains (Fig. 1A,B). A plausible explanation for this is that the adult and larval color patterns are, in many cases, regulated independently (Futahashi and Fujiwara, 2005; Futahashi et al., 2008), resulting in temporally different phenotypes from the same coding mutations. In addition to the melanic tissues, silkworm AANATs are also highly expressed in the anterior and middle silk gland (Fig. 2D), suggesting a potential pleiotropic role. The differential regulation of *Bm-iAANAT* in establishing pigmentation patterns in different tissues of larval and adult stages is intriguing, and the impact of *mln* phenotypes on the overall fitness of the mutants remains to be established.

Acknowledgements

We thank Drs Anjiang Tan, Hui Xiang, Xiaonan Yang and Yongzhen Xu for valuable discussions and Yajun Jiang for assistance with protein purification. The technical guidance of Jianhao Jiang and Sheng Wang was also greatly appreciated. This work was supported by the National Basic Research Program of China (2005CB121000), the National High-Tech R&D Program (2006AA10A119), and grants from the National Science Foundation of China (30825007 and 30174417).

Competing interests statement

The authors declare no competing financial interests.

Supplementary material

Supplementary material for this article is available at
http://dev.biologists.org/lookup/suppl/doi:10.1242/dev.053678/-/DC1

References

Andersen, S. O. (2005). Cuticular sclerotization and tanning. *Comprehensive Mol. Insect Sci.* **4**, 145-170.

Arakane, Y., Lomakin, J., Beeman, R. W., Muthukrishnan, S., Gehrke, S. H., Kanost, M. R. and Kramer, K. J. (2009). Molecular and functional analyses of amino acid decarboxylases involved in cuticle tanning in Tribolium castaneum. *J. Biol. Chem.* **284**, 16584-16594.

Ashida, M. and Brey, P. T. (1995). Role of the integument in insect defense: pro-phenol oxidase cascade in the cuticular matrix. *Proc. Natl. Acad. Sci. USA* **92**, 10698-10702.

Borjigin, J., Wang, M. M. and Snyder, S. H. (1995). Diurnal variation in mRNA encoding serotonin N-acetyltransferase in pineal gland. *Nature* **378**, 783-785.

Brodbeck, D., Amherd, R., Callaerts, P., Hintermann, E., Meyer, U. A. and Affolter, M. (1998). Molecular and biochemical characterization of the aaNAT1 (Dat) locus in Drosophila melanogaster: differential expression of two gene products. *DNA Cell Biol.* **17**, 621-633.

Carroll, S. B. (2005). Evolution at two levels: on genes and form. *PLoS Biol.* **3**, e245.

Duan, J., Li, R., Cheng, D., Fan, W., Zha, X., Cheng, T., Wu, Y., Wang, J., Mita, K., Xiang, Z. et al. (2010). SilkDB v2.0: a platform for silkworm (Bombyx mori) genome biology. *Nucleic Acids Res.* 38, D453-D456.

Elsik, C. G., Mackey, A. J., Reese, J. T., Milshina, N. V., Roos, D. S. and Weinstock, G. M. (2007). Creating a honey bee consensus gene set. *Genome Biol.* **8**, R13.

Ferry, G., Loynel, A., Kucharczyk, N., Bertin, S., Rodriguez, M., Delagrange, P., Galizzi, J. P., Jacoby, E., Volland, J. P., Lesieur, D. et al. (2000). Substrate specificity and inhibition studies of human serotonin N-acetyltransferase. *J. Biol. Chem.* **275**, 8794-8805.

Fujii, H., Banno, Y., Doira, H. and Kawaguchi, Y. (1998). *Genetical Stocks and Mutations of Bombyx mori: Important Genetic Resources*, 2nd edn. Fukuoka: Institute of Genetic Resources, Faculty of Agriculture, Kyusyu University.

Futahashi, R. and Fujiwara, H. (2005). Melanin-synthesis enzymes coregulate stage-specific larval cuticular markings in the swallowtail butterfly, Papilio xuthus. *Dev. Genes Evol.* **215**, 519-529.

Futahashi, R., Sato, J., Meng, Y., Okamoto, S., Daimon, T., Yamamoto, K., Suetsugu, Y., Narukawa, J., Takahashi, H., Banno, Y. et al. (2008). yellow and ebony are the responsible genes for the larval color mutants of the silkworm Bombyx mori. *Genetics* **180**, 1995-2005.

Gibert, J. M., Peronnet, F. and Schlotterer, C. (2007). Phenotypic plasticity in Drosophila pigmentation caused by temperature sensitivity of a chromatin regulator network. *PLoS Genet.* **3**, e30.

Goldsmith, M. R., Shimada, T. and Abe, H. (2005). The genetics and genomics of the silkworm, Bombyx mori. *Annu. Rev. Entomol.* **50**, 71-100.

Gompel, N., Prud'homme, B., Wittkopp, P. J., Kassner, V. A. and Carroll, S. B. (2005). Chance caught on the wing: cis-regulatory evolution and the origin of pigment patterns in *Drosophila*. *Nature* **433**, 481-487.

Hintermann, E., Grieder, N. C., Amherd, R., Brodbeck, D. and Meyer, U. A. (1996). Cloning of an arylalkylamine N-acetyltransferase (aaNAT1) from Drosophila melanogaster expressed in the nervous system and the gut. *Proc. Natl. Acad. Sci. USA* **93**, 12315-12320.

Huang, J., Zhang, Y., Li, M., Wang, S., Liu, W., Couble, P., Zhao, G. and Huang, Y. (2007). RNA interference-mediated silencing of the bursicon gene induces defects in wing expansion of silkworm. *FEBS Lett.* **581**, 697-701.

Ichihara, N., Okada, M. and Takeda, M. (2001). Characterization and purification of polymorphic arylalkylamine N-acetyltransferase from the American cockroach, Periplaneta americana. *Insect Biochem. Mol. Biol.* **32**, 15-22.

International Silkworm Genome Consortium (2008). The genome of a lepidopteran model insect, the silkworm Bombyx mori. *Insect Biochem. Mol. Biol.* **38**, 1036-1045.

Ito, K., Katsuma, S., Yamamoto, K., Kadono-Okuda, K., Mita, K. and Shimada, T. (2009). A 25bp-long insertional mutation in the BmVarp gene causes the waxy translucent skin of the silkworm, Bombyx mori. *Insect Biochem. Mol. Biol.* **39**, 287-293.

Ito, K., Katsuma, S., Yamamoto, K., Kadono-Okuda, K., Mita, K. and Shimada, T. (2010). Yellow-e determines the color pattern of larval head and tail spots of the silkworm Bombyx mori. *J. Biol. Chem.* **285**, 5624-5629.

Jeong, S., Rebeiz, M., Andolfatto, P., Werner, T., True, J. and Carroll, S. B. (2008). The evolution of gene regulation underlies a morphological difference between two Drosophila sister species. *Cell* **132**, 783-793.

Kan, H., Kim, C. H., Kwon, H. M., Park, J. W., Roh, K. B., Lee, H., Park, B. J., Zhang, R., Zhang, J., Soderhall, K. et al. (2008). Molecular control of phenoloxidase-induced melanin synthesis in an insect. *J. Biol. Chem.* **283**, 25316-25323.

Klein, D. C. (2007). Arylalkylamine N-acetyltransferase: 'the Timezyme'. *J. Biol. Chem.* **282**, 4233-4237.

Koch, P. B., Behnecke, B. and ffrench-Constant, R. H. (2000). The molecular basis of melanism and mimicry in a swallowtail butterfly. *Curr. Biol.* **10**, 591-594.

Kohn, M. H. and Wittkopp, P. J. (2007). Annotating ebony on the fly. *Mol. Ecol.* **16**, 2831-2833.

Lander, E. S., Green, P., Abrahamson, J., Barlow, A., Daly, M. J., Lincoln, S. E. and Newberg, L. A. (1987). MAPMAKER: an interactive computer package for constructing primary genetic linkage maps of experimental and natural populations. *Genomics* **1**, 174-181.

Maeda, T. (1939). Chiasma studies in the silkworm Bombyx mori. *Jpn. J. Genet.* **15**, 118-127.

Meng, Y., Katsuma, S., Mita, K. and Shimada, T. (2009a). Abnormal red body coloration of the silkworm, Bombyx mori, is caused by a mutation in a novel kynureninase. *Genes Cells* **14**, 129-140.

Meng, Y., Katsuma, S., Daimon, T., Banno, Y., Uchino, K., Sezutsu, H., Tamura, T., Mita, K. and Shimada, T. (2009b). The silkworm mutant lemon (lemon lethal) is a potential insect model for human sepiapterin reductase deficiency. *J. Biol. Chem.* **284**, 11698-11705.

Miao, X. X., Xub, S. J., Li, M. H., Li, M. W., Huang, J. H., Dai, F. Y., Marino, S. W., Mills, D. R., Zeng, P., Mita, K. et al. (2005). Simple sequence repeat-based consensus linkage map of Bombyx mori. *Proc. Natl. Acad. Sci. USA* **102**, 16303-16308.

Mita, K., Kasahara, M., Sasaki, S., Nagayasu, Y., Yamada, T., Kanamori, H., Namiki, N., Kitagawa, M., Yamashita, H., Yasukochi, Y. et al. (2004). The genome sequence of silkworm, Bombyx mori. *DNA Res.* **013**, 27-35.

Sakudoh, T., Iizuka, T., Narukawa, J., Sezutsu, H., Kobayashi, I., Kuwazaki, S., Banno, Y., Kitamura, A., Sugiyama, H., Takada, N. et al. (2010). A CD36-related transmembrane protein is coordinated with an intracellular lipid-binding protein in selective carotenoid transport for cocoon coloration. *J. Biol. Chem.* **285**, 7739-7751.

Soderhall, K. and Cerenius, L. (1998). Role of the prophenoloxidase-activating system in invertebrate immunity. *Curr. Opin. Immunol.* **10**, 23-28.

Tamura, K., Dudley, J., Nei, M. and Kumar, S. (2007). MEGA4: Molecular Evolutionary Genetics Analysis (MEGA) software version 4.0. *Mol. Biol. Evol.* **24**, 1596-1599.

True, J. R. (2003). Insect melanism: the molecules matter. *Trends Ecol. Evol.* **18**, 640-647.

True, J. R., Edwards, K. A., Yamamoto, D. and Carroll, S. B. (1999). Drosophila wing melanin patterns form by vein-dependent elaboration of enzymatic prepatterns. *Curr. Biol.* **9**, 1382-1391.

True, J. R., Yeh, S. D., Hovemann, B. T., Kemme, T., Meinertzhagen, I. A., Edwards, T. N., Liou, S. R., Han, Q. and Li, J. (2005). Drosophila tan encodes a novel hydrolase required in pigmentation and vision. *PLoS Genet.* **1**, e63.

Tsugehara, T., Iwai, S., Fujiwara, Y., Mita, K. and Takeda, M. (2007). Cloning and characterization of insect arylalkylamine N-acetyltransferase from Bombyx mori. *Comp. Biochem. Physiol.* **147**, 358-366.

Walter, M. F., Zeineh, L. L., Black, B. C., McIvor, W. E., Wright, T. R. and Biessmann, H. (1996). Catecholamine metabolism and in vitro induction of premature cuticle melanization in wild type and pigmentation mutants of Drosophila melanogaster. *Arch. Insect Biochem. Physiol.* **31**, 219-233.

Wittkopp, P. J., True, J. R. and Carroll, S. B. (2002a). Reciprocal functions of the Drosophila yellow and ebony proteins in the development and evolution of pigment patterns. *Development* **129**, 1849-1858.

Wittkopp, P. J., Vaccaro, K. and Carroll, S. B. (2002b). Evolution of yellow gene regulation and pigmentation in Drosophila. *Curr. Biol.* **12**, 1547-1556.

Wittkopp, P. J., Carroll, S. B. and Kopp, A. (2003a). Evolution in black and white: genetic control of pigment patterns in Drosophila. *Trends Genet.* **19**, 495-504.

Wittkopp, P. J., Williams, B. L., Selegue, J. E. and Carroll, S. B. (2003b). Drosophila pigmentation evolution: divergent genotypes underlying convergent phenotypes. *Proc. Natl. Acad. Sci. USA* **100**, 1808-1813.

Wittkopp, P. J., Stewart, E. E., Arnold, L. L., Neidert, A. H., Haerum, B. K., Thompson, E. M., Akhras, S., Smith-Winberry, G. and Shefner, L. (2009). Intraspecific polymorphism to interspecific divergence: genetics of pigmentation in Drosophila. *Science* **326**, 540-544.

Wray, G. A. (2007). The evolutionary significance of cis-regulatory mutations. *Nat. Rev. Genet.* **8**, 206-216.

Wright, T. R. (1987). The genetics of biogenic amine metabolism, sclerotization, and melanization in Drosophila melanogaster. *Adv. Genet.* **24**, 127-222.

Xia, Q., Zhou, Z., Lu, C., Cheng, D., Dai, F., Li, B., Zhao, P., Zha, X., Cheng, T., Chai, C. et al. (2004). A draft sequence for the genome of the domesticated silkworm (Bombyx mori). *Science* **306**, 1937-1940.

Xia, Q., Cheng, D., Duan, J., Wang, G., Cheng, T., Zha, X., Liu, C., Zhao, P., Dai, F., Zhang, Z. et al. (2007). Microarray-based gene expression profiles in multiple tissues of the domesticated silkworm, Bombyx mori. *Genome Biol.* **8**, R162.

Yamamoto, K., Nohata, J., Kadono-Okuda, K., Narukawa, J., Sasanuma, M., Sasanuma, S. I., Minami, H., Shimomura, M., Suetsugu, Y., Banno, Y. et al. (2008). A BAC-based integrated linkage map of the silkworm Bombyx mori. *Genome Biol.* **9**, R21.

Zhan, S., Huang, J., Guo, Q., Zhao, Y., Li, W., Miao, X., Goldsmith, M. R., Li, M. and Huang, Y. (2009). An integrated genetic linkage map for silkworms with three parental combinations and its application to the mapping of single genes and QTL. *BMC Genomics* **10**, 389.

Table S1. Primers (5′ to 3′) used

Name	Forward	Reverse
S1801	GGTAAGGGCAGTGCTTTGTAGAATC	TGCGGAACCACTCACAAACTT
S1802	CGCTTACGGAGGTCCATGAGG	CGCTTTTACCGATAAGACCGCT
S1806	TGCTGAAGGACAAAAGGGAATG	CATTGTGGATGTCTACGGGCTC
S1807	TTTATTTGTTAGGCTCGTTACTGTCA	CAAAAGCACAGCTACTTCCGC
S1808	CCGAGTAGAACTGCGCTAATGTACTT	GGGTCTGCGACGGCGAT
S1809	GCTTTAGCGATAAGACCGCCTATT	TCACTGACCGAAGCGGAAAC
S1811	TTTTCCTAGTTCAGTTGTAAAGCGAT	GCAAAGTAGAGGGGAAGAGGTCG
S1812	CGTCATAGCAGTAAATAACCCGC	GGAACTTATACACGCCTTTTCATCT
C1_1	TCAGACCAAGCATCATCCG	AAGGCGGTGAATGGCAAC
C1_2	TTATTACAGAGGAGCGACTGC	ACCACAATGCTAAGGGTTGA
C2_1	TAGATGGCGGGAGTGGAC	CACTCCAAAGGACCAATTAAG
C2_2	GTCAGGTTTATCATCAGTTGCTTAG	TGGCACCCTAATTTTTGG
C3	TTCTTGCTCTGTCAAGGTCAT	GGTTTGCTTCCAGTACGCT
C6	GTGTTTGCTTTCACCCTTTC	CCCCCAGCCCTACACTATC
C7	TAACTATACCATCGTGAATCCG	AACTAGCTGTACCCGTCCG
C8	GAGGTAGGTGGCGGCTTTT	CGTTACAGGACGGAACATTTAT
C11	CAAACTGAACATCGCCAAAT	GCACGGCCCTCTACCTTA
C12_1	GACATTCCTAACACCCACCG	CGATACTTACTCCGTTTCTCTCA
C12_2	ACAAGATTCTCGTTTCGGACC	TTCGCAGACACTGGAAAAGGTA
C13	CTGGTTGTACTCGGCACG	CCCCTACACACCCTTGGA
Fig3C	CGCAAAATGTCCGTTCCA	GCAAATCAGCATACCGAACC
RT_C11	CCTCGCAAAATGTCCGTT	TTTGGATTGGGGCAGTCT
RT_C12	ATTCTTCATCGACGAACCCT	CTCCTCATCTTCATCCTCCAA
RT_G3	GGCAGATAAACAGCCAAAGA	CTGGAACAGCAACAACATTAGA

Table S2. Detailed information on 13 predicted genes (C1-C13) within the candidate regions and reasons for further screening or otherwise

Candidate	Gene name*	Length (bp)	Annotation: best hit with E-value	Exclusion reason
C1	BGIBMGA008531	303	Myb-MuvB complex subunit Lin-52 [*B. mori*] (E-value: 2.00E–39)	Two *Dazao*-specific SNPs
C2	BGIBMGA008532	564	N-acetyltransferase [*B. mori*] (E-value: 5.00E–103)	Identical to *Dazao*
C3	BGIBMGA008324	246	AGAP002567-PA [*A. gambiae*] (E-value: 8.00E–05)	Two silent SNPs
C4	BGIBMGA008533	1326	Similar to AGAP001885-PA [*T. castaneum*] (E-value: 3.00E–90)	Irrelevant expression pattern
C5	BGIBMGA008323	249	Hypothetical protein SS1G_04978 [*S. sclerotiorum*] (E-value: 4.3)	Irrelevant expression pattern
C6	BGIBMGA008322	216	Similar to GA18100-PA [*N. vitripennis*] (E-value: 2.00E–20)	Three silent SNPs
C7	BGIBMGA008534	1116	GK25744 [*D. willistoni*] (E-value: 6.00E–110)	Non-*mln*-specific insertion; irrelevant expression pattern
C8	BGIBMGA008535	252	Snrnp48 protein [*D. rerio*] (E-value: 1.2)	One *Dazao*-specific SNP; one *Dazao*-specific deletion
C9	BGIBMGA008536	1131	Similar to zinc-finger CCCH-type containing 14 [*T. castaneum*] (E-value: 4.00E–27)	Irrelevant expression pattern
C10	BGIBMGA008537	1350	Conserved hypothetical protein [*C. quinquefasciatus*] (E-value: 3.00E–33)	Irrelevant expression pattern
C11	BGIBMGA008538	787	Arylalkylamine N-acetyltransferase [*B. mori*] (E-value: 2.00E–107)	*mln*-specific 126 bp deletion; coincident expression pattern
C12	BGIBMGA008539	660	Arylalkylamine N-acetyltransferase [*A. pernyi*] (E-value: 3.00E–30)	Identical to *Dazao*
C13	BGIBMGA008540	390	Similar to AGAP003014-PA [*T. castaneum*] (E-value: 1.00E–28)	Identical to *Dazao*

*Duan et al. (2010).

Table S3. Raw radiolabel values detected in the AANAT enzymatic assays (tryptamine as substrate)

		Reaction time (minutes)			
Proteins	Amount (ng)	5	10	15	20
wt in DE3	10	453.3	728.3	582.3	1101.7
	20	1148.7	1895.3	2605.3	2874
	30	1357.7	2351	3043.3	4017.7
wt in Sf9	20	1092.3	1759	2172	3207.7
	30	2016.7	2648.3	3882.7	4238.3
lm in Sf9	20	149	136	130.5	114.5
	30	160.75	159	166.25	114.5
sm in DE3	10	183.7	214.3	210.7	223.3
	20	225	243.3	298	304.7
	30	232.7	294.3	369.7	494.3
Ctrl 1*	–	141.3	141.7	160.3	144.3
Ctrl 2†	–	141.7	143.7	155.3	144.3

*No tryptamine/dopamine.
†Tryptamine/dopamine added.

Table S4. Raw radiolabel values detected in the AANAT enzymatic assays with dopamine as substrate and a 20-minute reaction time

Proteins	Amount (ng)	Radiolabel values
wt in DE3	10	2339
	20	4282
	30	6992.5
sm in DE3	10	1373
	20	1526
	30	1852.5
Ctrl 1*	–	1071
Ctrl 2†	–	1190

*No tryptamine/dopamine.

†Tryptamine/dopamine added.

Table S5. Phenotypic counts for the C12 RNAi experiment

Treatment	Gender	Injected	Molted				Death
			Total	R	O	No	
dsC12 (10 μg)	All	178	175	0	0	175	3
	Male	93	91	0	0	91	2
	Female	85	84	0	0	84	1
dsC12 (15 μg)	All	92	87	0	0	87	5
	Male	43	39	0	0	39	4
	Female	49	48	0	0	48	1
dsEGFP	All	87	85	0	0	85	2

R, regional melanization; O, overall melanization; No, no ectopic phenotype.